Extended View Tables and Figures

Yeast strains

Yeast strains harboring a deletion in genes encoding for specific SWI/SNF subunits were obtained from the yeast gene deletion collection MATa library (Open Biosystems). For purification, another subunit (as indicated in Figure. 1) was tagged at the C terminus with a double FLAG epitope by standard methods. Genotypes were verified by PCR and sequencing. A list of strains used in this study is provided below:

Strain name as described in the figures and text	Description	Genotype
WT - 1	BY4742 parental background, *Snf6* tagged with FLAG-LEU2 and *Swi3* tagged with HA-V5-His6-KanMX4	*matα his3Δ1 leu2Δ0 lys2Δ0 ura3Δ0 swi3::swi3-HA-V5-His6-kanMX4 snf6::snf6-FLAG-LEU2*
WT - 2	BY4741 parental background, *Snf2* tagged with 2FLAG-LEU2	*mata his3Δ1 leu2Δ0 met15Δ0 ura3Δ0 snf2::snf2-2FLAG-9 amino acids-LEU2*[1]
Δsnf2	BY4741 parental background, *Snf2* replaced with KanMX4 and *Snf6* tagged with 2FLAG-LEU2	*mata his3Δ1 leu2Δ0 met15Δ0 ura3Δ0 snf2Δ::kanMX4 snf6::snf6-2FLAG-9 amino acids-LEU2*[1]
Δsnf5	BY4741 parental background, *Snf5* replaced with KanMX4 and *Snf6* tagged with 2FLAG-LEU2	*mata his3Δ1 leu2Δ0 met15Δ0 ura3Δ0 snf5Δ::kanMX4 snf6::snf6-2FLAG-9 amino acids-LEU2*[1]
Δsnf6	BY4741 parental background, *Snf6* replaced with KanMX4 and *Swp73* tagged with 2FLAG-LEU2	*mata his3Δ1 leu2Δ0 met15Δ0 ura3Δ0 snf6Δ::kanMX4 swp73::swp73-2FLAG-9 amino acids-LEU2*[1]
Δswp82	BY4741 parental background, *Swp82* replaced with KanMX4 and *Snf6* tagged with 2FLAG-LEU2	*mata his3Δ1 leu2Δ0 met15Δ0 ura3Δ0 swp82Δ::kanMX4 snf6::snf6-2FLAG-9 amino acids-LEU2*[1]

[1]The 9 amino acid insertion has the sequence 5′ gtc gac tct aga gga tcc ccg ggt acc 3′ and translates to VDSRGSPGT.

Table EV1. Related to Figures 1 and 4. Listing of all the interlinks observed in yeast SWI/SNF.

When 2 and 5 mM BS3 was used, respectively 332 and 322 interlinks were confidently identified and under both these conditions 207 were identified. No obvious condition-specific crosslinking patterns were detected, rather these differences are likely due to under sampling during shotgun mass spectrometry. Altogether 447 interlinks were identified. The raw CX-MS data will be deposited at PRIDE upon acceptance of the manuscript.

See attached file

Table EV2. Related to Figures 1 and 4. Listing of all the intralinks observed in yeast SWI/SNF

When 2 and 5 mM BS3 were used, respectively 548 and 468 intralinks were confidently identified and 356 intralinks were identified under both conditions. Altogether 659 intralinks were identified. Since there are two copies of Swi3 in the SWI/SNF complex, some of the identified intralinks may actually be crosslinks between two molecules of the same subunit. We cannot distinguish between these two possibilities based on the CXMS data alone. See attached file

Table EV3. Related to Figure 5. Kinetic parameters obtained from Michaelis-Menten analysis[1]

Protein	WT-array	Δsnf5 - array	WT - NCP	Δsnf5 - NCP	WT-DNA	Δsnf5 - DNA
K_M (μM)	135 ± 20	182 ± 57	110 ± 30	110 ± 54	98 ± 24	78 ± 13
k_{cat} (min^{-1})	575 ± 31	209 ± 27	670 ± 76	329 ± 68	419 ± 43	249 ± 15
k_{cat}/K_M (μM^{-1} min^{-1})	4.3	1.1	6.1	3	4.3	3.2

[1]Under multiple turnover conditions (saturation amount of nucleosomes)

Table EV4. Related to Figure 7. GO terms analysis of genes affected by the loss of Snf5

Down regulated by loss of Snf5

Description	P-value	FDR q-value	Enrichment
transposition, RNA-mediated	4.13E-23	2.03E-19	18.32
DNA integration	8.47E-22	2.08E-18	17.94
transposition	1.74E-21	2.85E-18	16.08
DNA recombination	2.41E-09	2.97E-06	4.1
siderophore transport	7.45E-08	6.11E-05	20.93
iron chelate transport	7.45E-08	7.33E-05	20.93
iron coordination entity transport	1.53E-07	1.08E-04	14.65
iron ion homeostasis	4.13E-06	2.54E-03	6.04
ion transport	5.47E-05	2.99E-02	2.65

Up regulated by loss of Snf5

Description	P-value	FDR q-value	Enrichment
methionine metabolic process	1.61E-10	7.94E-07	11.68
methionine biosynthetic process	4.10E-10	1.01E-06	12.55
sulfur compound biosynthetic process	8.05E-10	1.32E-06	11.87

alpha-amino acid metabolic process	1.81E-09	2.23E-06	4.99
small molecule biosynthetic process	5.54E-09	5.45E-06	3.64
alpha-amino acid biosynthetic process	6.32E-09	5.18E-06	5.97
cysteine metabolic process	8.07E-09	5.67E-06	21.5
aspartate family amino acid biosynthetic process	4.13E-08	2.54E-05	8.44
aspartate family amino acid metabolic process	4.92E-08	2.69E-05	7.37
carboxylic acid biosynthetic process	5.04E-08	2.48E-05	4.33
hydrogen sulfide biosynthetic process	5.40E-08	2.42E-05	33.27
hydrogen sulfide metabolic process	5.40E-08	2.21E-05	33.27
sulfur compound metabolic process	8.91E-08	3.37E-05	5.35
cysteine biosynthetic process	9.25E-08	3.25E-05	21.78
sulfate assimilation	9.25E-08	3.03E-05	21.78
organic acid biosynthetic process	1.04E-07	3.20E-05	4.14
cellular amino acid biosynthetic process	1.13E-07	3.28E-05	5.25
serine family amino acid metabolic process	1.22E-07	3.33E-05	10.27
cellular amino acid metabolic process	3.64E-07	9.41E-05	3.66
serine family amino acid biosynthetic process	1.29E-06	3.17E-04	11.64
sulfur amino acid metabolic process	2.19E-06	5.13E-04	14.09
hexose transmembrane transport	4.06E-06	9.08E-04	9.98
organic acid metabolic process	5.76E-06	1.23E-03	2.57
thiamine-containing compound biosynthetic process	6.31E-06	1.29E-03	16.63
thiamine biosynthetic process	6.31E-06	1.24E-03	16.63
carbohydrate transmembrane transport	6.69E-06	1.27E-03	9.32
oxidation-reduction process	7.68E-06	1.40E-03	2.59
glucose import	8.47E-06	1.49E-03	9.01
small molecule metabolic process	8.81E-06	1.49E-03	2.09

Table EV5. Related to Figure 7. Listing of all GO term analysis

please see enclosed

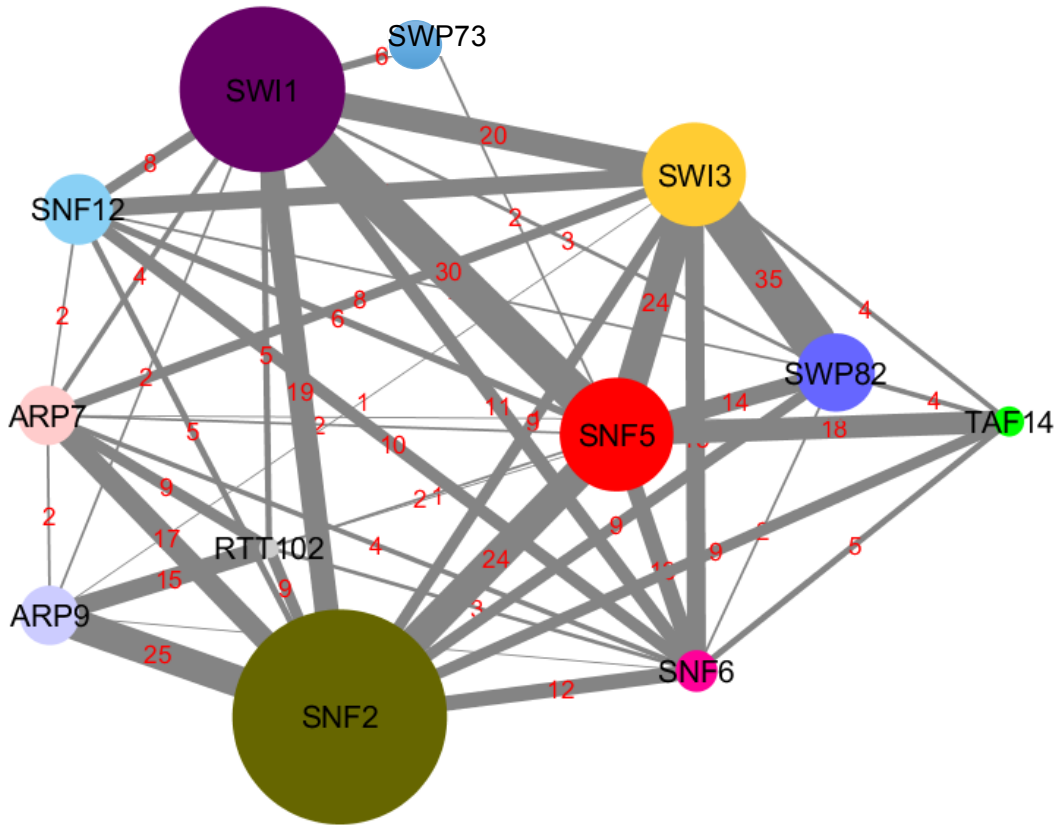

Figure EV1. Related to Figures 1 and 4. Summary of the crosslinks for the SWI/SNF complex.

447 interlinks were identified between SWI/SNF subunits. The width of the edges indicates the number of crosslinks identified between the two subunits. The size of the subunit is proportion to its length. The protein-protein interactions (PPIs) revealed by this map are consistent with much of our understanding of the SWI/SNF PPI network. First, the core and most evolutionarily conserved SWI/SNF subunits are heavily interconnected: SNF2 (SMARCA2/Brm and SMARCA4/Brg1 in humans), SWI1 (ARID1A and ARID1B in humans), SWI3 (SMARCC1 and SMARCC2 in humans) and SNF5 (SMARCB1/INI1 in humans). This suggests that these subunits interact with each other to form an evolutionarily conserved scaffold in the SWI/SNF complex, while the other subunits that interact with the core can vary in composition, conservation, and stoichiometry in different organisms, or in different cell types in higher organisms. This organization of the SWI/SNF complex may facilitate condition- or cell type-specific changes in subunit composition in higher organisms. Second, and consistent with previous results (Schubert et al., 2013), the actin-like module consisting of Arp7, Arp9 and Rtt102 forms a tight submodule that interacts with Snf2. In fact, the crosslinks to the HSA domain of Snf2 agree well with the crystal structure of the submodule (Figure EV4). Third, there is strong connectivity between Snf5 with core subunits as well as with Swp82 and Taf14. Taf14 interacts with Snf5 by far western analysis using ^{35}S-labeled Taf14 (Cairns et al., 1996).

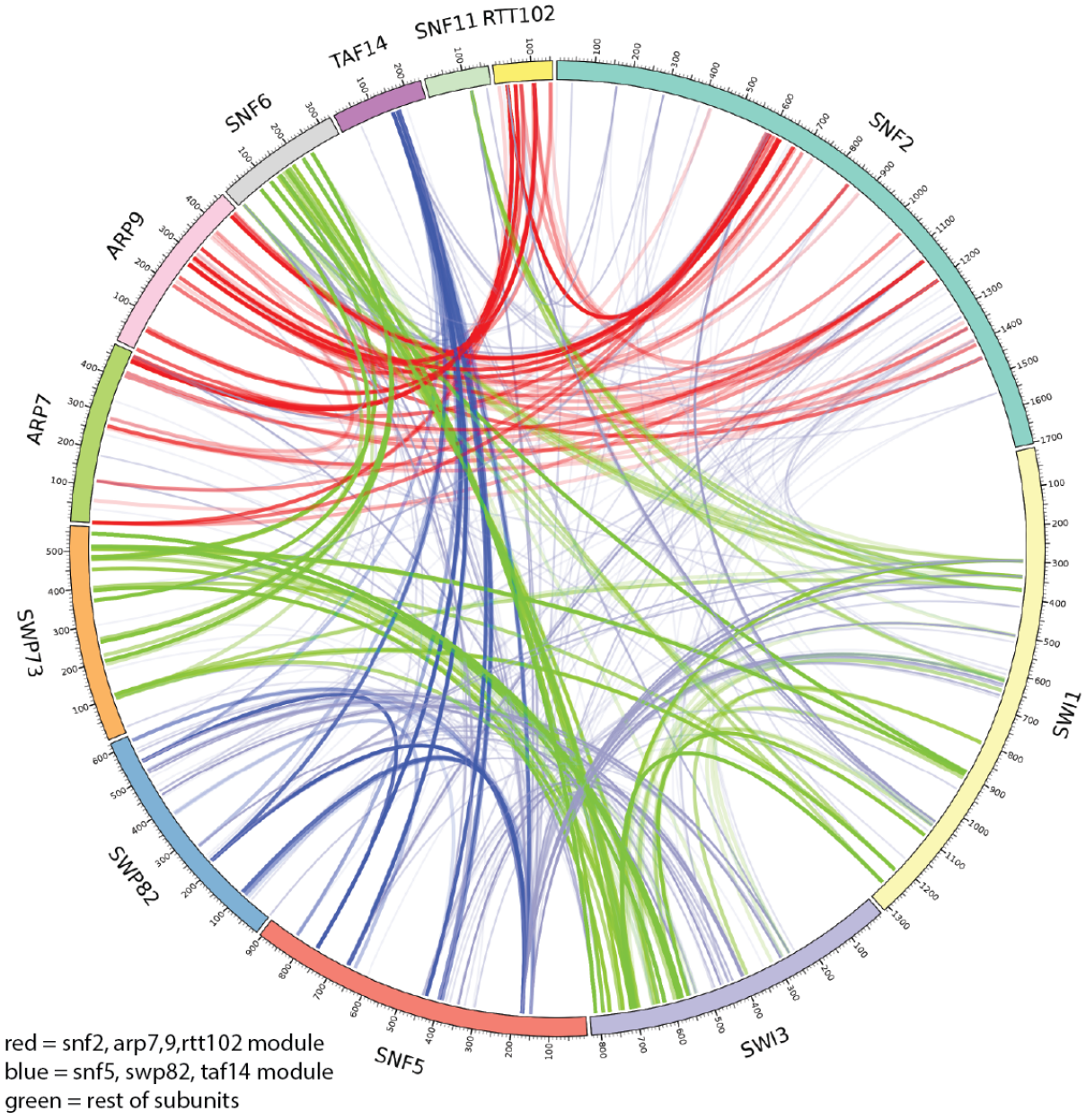

Figure EV2. Related to Figures 1 and 4. BS3 crosslinks between the subunits of the SWI/SNF complex (total 447).

The polypeptide chain of each subunit is represented as a segment of this circle with different colors. The thickness and intensity of each line corresponds to the number of crosslinks observed between the corresponding regions. Lines are color coded as indicated.

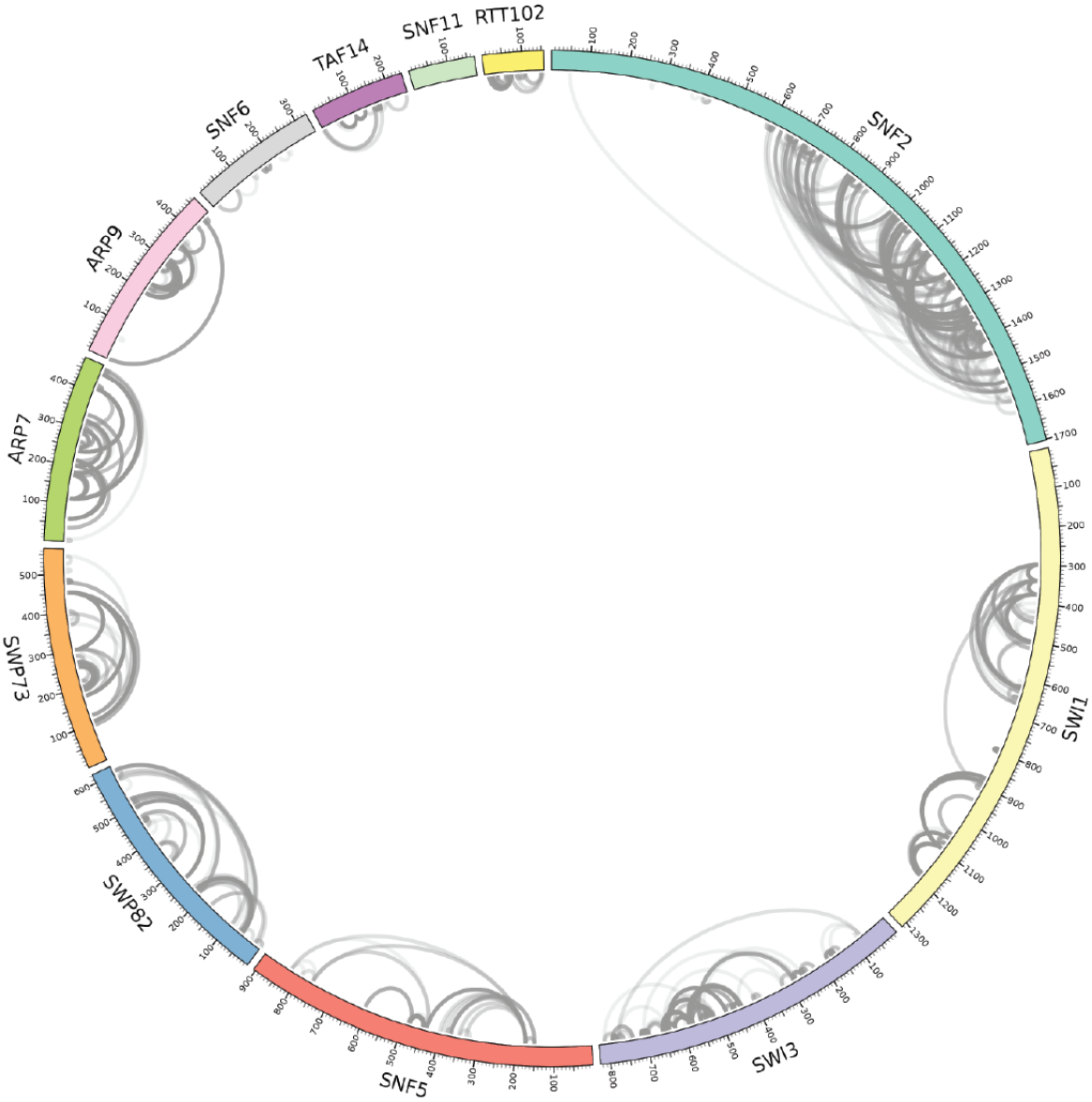

Figure EV3. Related to Figures 1 and 4. BS intralinks for all of the subunits of the SWI/SNF complex (total 659).

The subunits of SWI/SNF are presented the same as in Figure EV2, except that only intralinks are shown as gray lines.

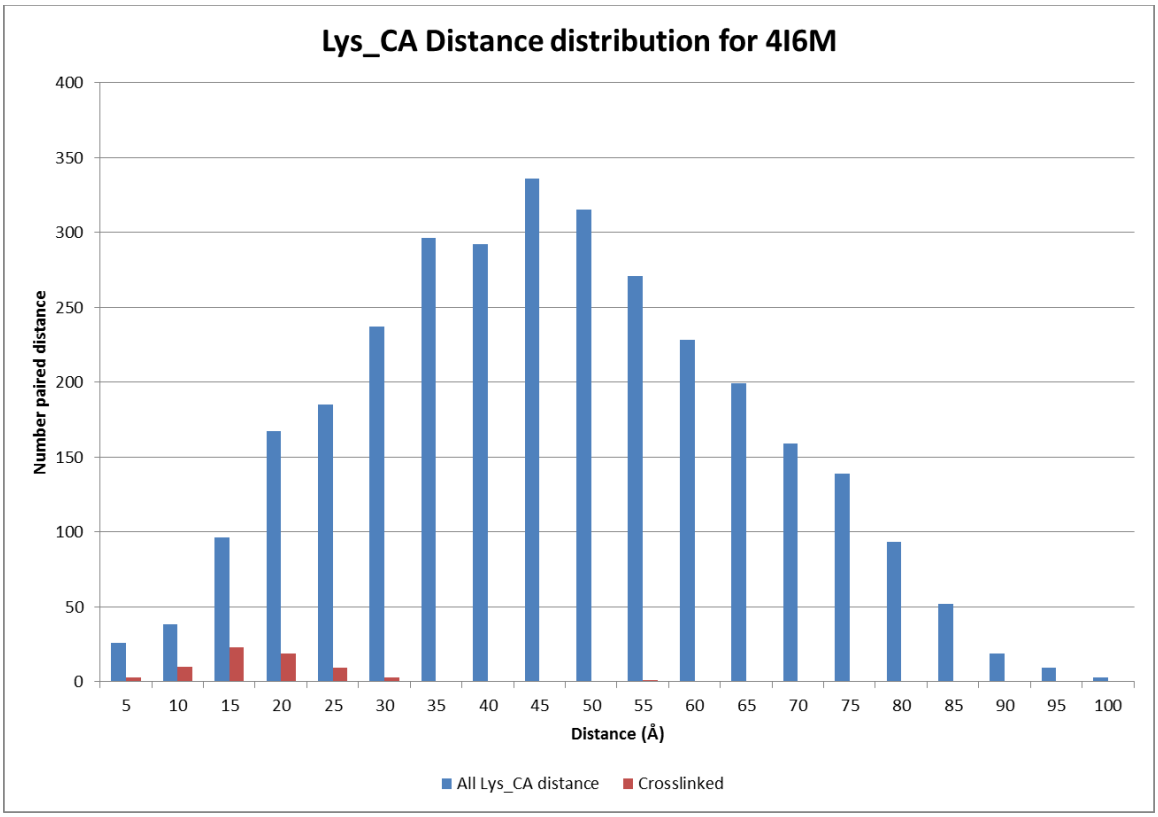

Figure EV4. Related to Figures 1 and 4. Cα distance distribution of the Lys residues in the Arp7-Arp9-Snf2(HSA)-Rtt102 sub-complex.

To evaluate the utility of the data for studying the subunit organization of SWI/SNF, we mapped the positions of crosslinked lysine residues onto available crystal structures or homology models of SWI/SNF subunits/domains and measured the alpha carbon (Cα) distance between the crosslinked residues. All of the Lys residues in the Arp7-Arp9-Snf2(HSA)-Rtt102 complex (4i6m.pdb) are depicted by blue bars; whereas the Cα distance distribution for all identified crosslinked residues that could be mapped onto the Arp7-Arp9-Snf2(HSA)-Rtt102 structure are depicted by red bars. BS3 has a linker arm of 11.4 Å when fully extended and can crosslink two lysine residues whose Cα atoms are up to 30 Å apart (Merkley et al., 2014). 67 crosslinked pairs were mapped onto the Arp7-Arp9-Snf2(HSA)-Rtt102 sub-complex structure (4i6m.pdb), and all of the Cα distances are $\leq$ 30 Å (Figure EV4). We generated a homology model of the Snf2 helicase domain using Modeller 9.9 (Sali and Blundell, 1993) and the Rad54 helicase (1Z3I.pdb) as template. Out of 85 intralinks that were mapped onto the model, 60 are within the theoretical crosslinking distance of BS3. For the 25 crosslinks with distances larger than 34 Å, at least one of the crosslinked residues is in a flexible region in the modeled structure. These results indicate that our crosslinking data provides reliable distance restraints that are useful for studying the architecture of SWI/SNF.

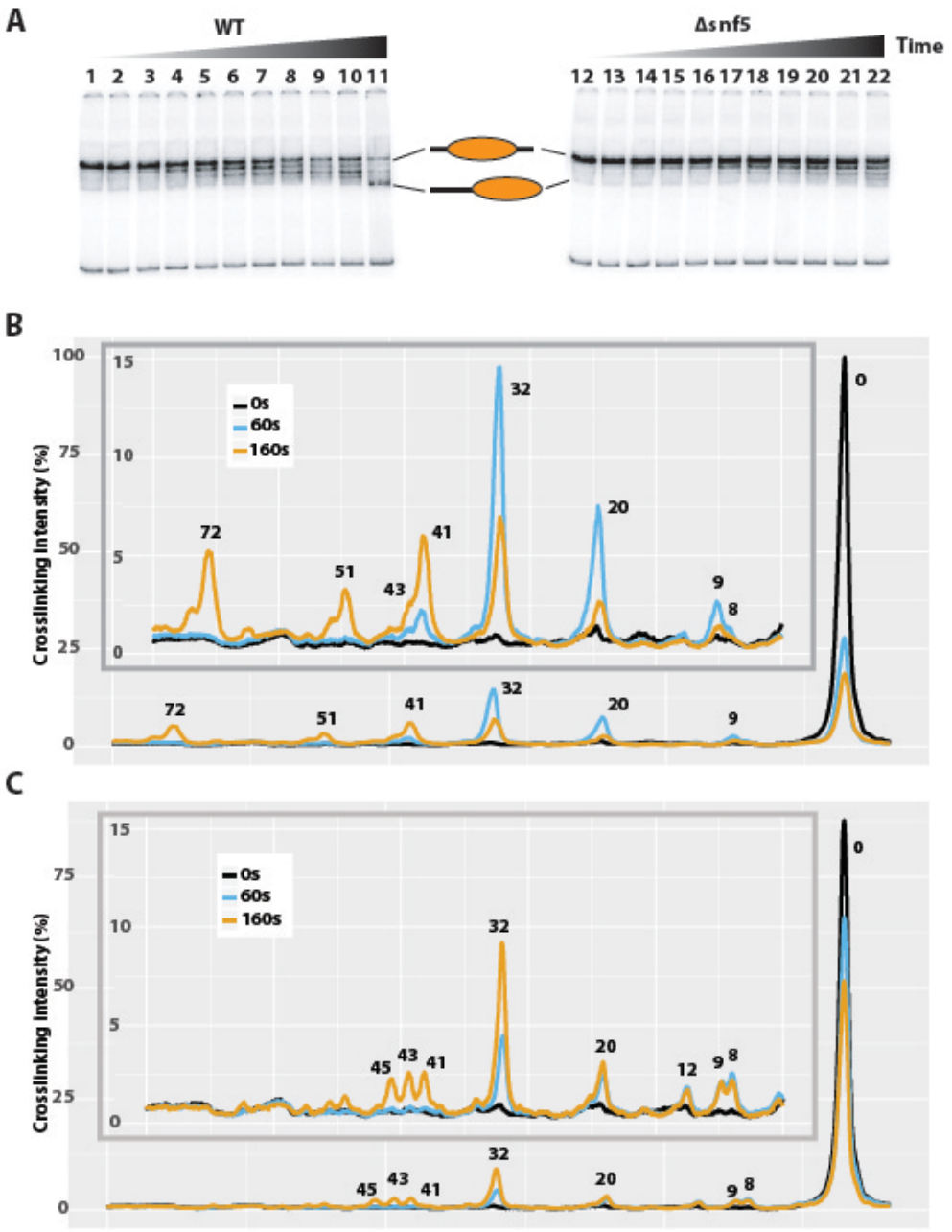

Figure EV5. Related to Figure 6. Loss of Snf5 causes SWI/SNF to pause more when moving nucleosomes.

(A) Saturating amounts of WT SWI/SNF (lanes 1-11) and Δsnf5 complexes (lanes 12-22) were used to remodel radiolabeled centrally positioned 29N59 nucleosomes for 0,5,10,20,30,40,50,60,70,80 and160s. Remodeled nucleosomes were separated on a 5% native PAGE after removing bound remodeler and visualized by autoradiography. **(B-C)** The lanes from the gel image shown in Figure 7A and B were quantitated, normalized and plotted for three different time points (0,60 and 160 s) with WT (B) and Δsnf5 complex (C). The numbers above each peak indicate the number of nucleotides (nt) moved from the starting cleavage position (0).

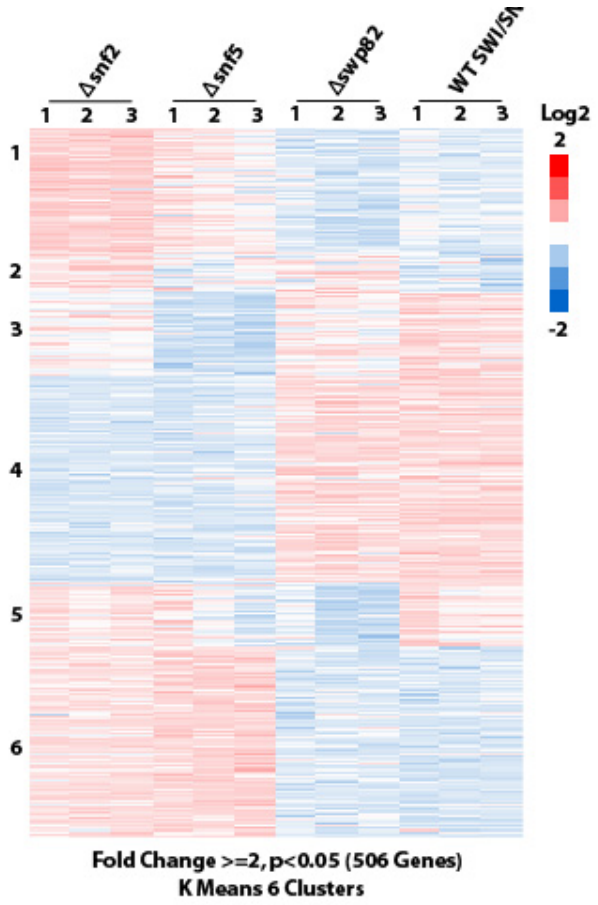

Figure EV6. Related to Figure 7. Biological replicates for RNA-seq analysis of Δsnf5, Δsnf2, Δswp82 and wild type SWI/SNF.
Genes were filtered either by expression profile satisfying fold change >= 2 and $p < 0.05$ - 506 genes. Genes were clustered into 6 groups using K-means with red representing activated and blue repressed genes.

References

Cairns, B.R., Henry, N.L., and Kornberg, R.D. (1996). TFG/TAF30/ANC1, a component of the yeast SWI/SNF complex that is similar to the leukemogenic proteins ENL and AF-9. Mol Cell Biol *16*, 3308-3316.
Merkley, E.D., Rysavy, S., Kahraman, A., Hafen, R.P., Daggett, V., and Adkins, J.N. (2014). Distance restraints from crosslinking mass spectrometry: mining a molecular dynamics simulation database to evaluate lysine-lysine distances. Protein Sci *23*, 747-759.
Sali, A., and Blundell, T.L. (1993). Comparative protein modelling by satisfaction of spatial restraints. J Mol Biol *234*, 779-815.
Schubert, H.L., Wittmeyer, J., Kasten, M.M., Hinata, K., Rawling, D.C., Heroux, A., Cairns, B.R., and Hill, C.P. (2013). Structure of an actin-related subcomplex of the SWI/SNF chromatin

remodeler. Proceedings of the National Academy of Sciences of the United States of America *110*, 3345-3350.